

Leading corrections to local approximations

Attila Cangi, Donghyung Lee, Peter Elliott, and Kieron Burke

Departments of Chemistry and of Physics, University of California, Irvine, CA 92697, USA

(Dated: November 21, 2018)

For the kinetic energy of 1d model finite systems the leading corrections to local approximations as a functional of the potential are derived using semiclassical methods. The corrections are simple, non-local functionals of the *potential*. Turning points produce quantum oscillations leading to energy corrections, which are completely different from the gradient corrections that occur in bulk systems with slowly-varying densities. Approximations that include quantum corrections are typically much more accurate than their local analogs. The consequences for density functional theory are discussed.

I. INTRODUCTION

Modern density functional theory (DFT) has become a popular electronic structure method, because of its balance between computational efficiency and accuracy. The original density functional theory was that of Thomas¹ and Fermi² (TF), in which all parts of the electronic Hamiltonian are approximated by explicit density functionals, and the energy minimized over possible densities. Typical errors in TF theory are of order 10% of the total energy, but molecules don't bind.³ In the 1950's, Slater⁴ introduced the idea of *orbitals* in DFT, i.e., solving a set of single-particle equations to construct the energy of the interacting system, which is typically much more accurate. This was shown to be a formally exact approach in the celebrated works of Hohenberg and Kohn⁵ and Kohn and Sham.⁶ The latter also introduced the local density approximation (LDA) for the only unknown needed to solve the Kohn-Sham (KS) equations, the exchange-correlation (XC) energy as a functional of the density. Since then, the field has gradually evolved with improvements in computational power, algorithms, and approximate functionals to the workhorse it is today.⁷

Unfortunately, the existence theorems give no hint of how to construct approximate functionals. Presently, there is a dazzling number of such approximate functionals suggested in the literature, and implemented in standard codes, both in physics and chemistry.⁸ Many of these are physically motivated, and work well for the systems and properties for which they were designed, but usually fail elsewhere. There appears to be no systematic approach to the construction of these functionals, beyond artful constraint satisfaction.⁹

In the present paper, we return to the origins of DFT and ask, what are the leading corrections to the original approximation of Kohn and Sham, the LDA? This is a very difficult question that we can only aspire to answer for the XC energy for any electronic system. In the present article, we answer the question for an extremely simple case, but one that contains many features relevant to the problems of electronic structure.

The original works on density functional approximations emphasize the gradient expansion,^{5,6} which is a particular approach to improve upon a local density approximation. Imagine an infinitely extended slowly-varying

gas. The corrections to the local approximation are given accurately by leading corrections in the density gradient. But real systems do not look like slowly-varying gases. All finite systems have evanescent regions, as do many bulk solids. The regions can be separated via classical turning-point surfaces, evaluated at the Fermi energy of the system.¹⁰ Typically, such regions are atomic sized. Most importantly, the gradient expansion fails completely both near and outside these surfaces. Generalized gradient approximations (GGAs) and other methods have been developed to overcome these difficulties. These include only a finite order of gradients, but employ a form which contains many powers those gradients.

To study the effects of confinement to finite regions on density functional approximations, we use non-interacting particles, and study only their kinetic energy, which was locally approximated in the original TF theory. We study only one dimension, where semiclassical approximations are simple, and the WKB¹¹⁻¹³ form applies in the absence of classical turning points where the potential $v(x)$ has finite slope. We avoid such turning points by using box boundary conditions and studying only systems whose chemical potential is everywhere above $v(x)$.

The answer is surprising: For most systems, the leading corrections (in a sense that will become clear within) are *not* the simple gradient corrections commonly discussed, and used as starting points to construct GGAs. Instead, both the density and kinetic energy density can be very accurately approximated as functionals of the *potential*.

The limit we discuss is also an important result in itself. We carefully show precisely how TF becomes exact in a semiclassical limit. Essentially, we take $\hbar \rightarrow 0$, keeping the chemical potential μ roughly fixed, and renormalizing the density so as to retain the original particle number. If, further, one performs a moving-average over the space coordinate, with a range chosen to be small compared to the spatial variation of the potential, but large compared to quantum oscillations as $\hbar \rightarrow 0$, the density uniformly converges to that of TF theory. We call this the continuum limit of a *finite* system. The separation between quantum eigenvalues becomes infinitesimal, and all sums become integrals. The integrands within contain purely classical quantities in terms of the potential, $v(x)$. A similar simplification occurs for the kinetic en-

ergy density, given in terms of $v(x)$, and when $v(x)$ is eliminated from the two expressions, what remains is the LDA to the kinetic energy.

Having carefully defined this limit, we can then discuss the approach to that limit, and the leading corrections to the local approximation. We find that the dominant corrections (in $1/\hbar$) are *not* gradient corrections due to the variations in $v(x)$ in the interior, but rather are quantum oscillations due to the hard walls at the boundaries. These quantum oscillations are generic features of any quantum system, and their nature is determined by the classical turning points.¹⁴ They give rise to the phase corrections to the classical density of states in the Gutzwiller trace formula,¹⁵ and will be present for *any* finite quantum system. The only case in which they vanish is that of periodic boundary conditions with the chemical potential above the maximum of the potential. Only in such systems does the gradient expansion produce the correct asymptotic expansion in powers of \hbar , equivalent to gradients of the potential. For any finite system, the series eventually diverges, but truncation at a lower order can yield highly accurate results, if the gradients are sufficiently small.

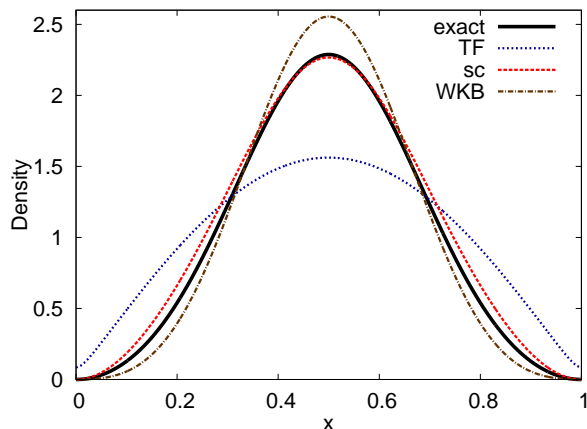


FIG. 1: Exact, TF, our semiclassical (sc), and WKB density for a single particle in $v(x) = -12 \sin^2(\pi x)$ with hard walls at $x = 0$ and $x = 1$ ($\hbar = m = 1$).

To give some idea of the power of the methods we develop, in Fig. 1 we show the density of one particle in a simple well ($v(x) = -D \sin^2(\pi x/L)$ in a box from 0 to L , with $D = 12$.) The exact density is found by numerically solving the Schrödinger equation. The TF density is found by minimizing the 1d TF kinetic energy functional and choosing the chemical potential to yield one particle. That density smoothly follows the potential. Due to the hard walls there are no classical turning points where $v(x)$ has finite slope. Hence, a WKB treatment can be applied here, yielding a WKB eigenvalue that is positive and reasonably accurate. But the result of our present analysis is a simple formula for the density, which uses WKB wavefunctions as input, is much more accurate

still. Perhaps more importantly, we have been unable to create situations where our approximation completely fails.

In the electronic structure problem, the local approximation to the XC energy is analogous to the TF approximation in Fig. 1. While there are many excellent approximations that improve over the local approximation by typically an order of magnitude, they are usually tailored to specific systems or properties, and contain either empirical parameters¹⁶ or at least careful selection of exact conditions to impose on an approximation to fix the parameters non-empirically.¹⁷ Our formulas are derived via a semiclassical analysis that yields unique approximations, are robust, and typically *two* orders of magnitude better than the local approximation.

The semiclassical result for the density was given in a short report¹⁸, but the kinetic energy density formula derived there failed close to the boundaries. Here we explain that failure, in terms of boundary-layer theory^{19,20}, but applied to sums over eigenstates rather than individual solutions to a differential equation. By identifying our limit, we can then cleanly separate the two different length scales in the problem. Earlier approaches^{14,21} yield only the asymptotic result in the interior of the system (ironically labelled the outer region in boundary layer theory), but that there exists a region close to each wall (appropriately called a boundary layer) where that solution fails. However, within the boundary layer, a different asymptotic expansion applies and, by matching these two solutions, we construct a *uniform* approximation that is asymptotic to a given order *everywhere* in the system. Many different aspects of these issues have been addressed over the decades since the original work of Kohn and Sham.¹⁴ For example, Balian and Bloch,²² in the context of nuclear physics, identified the need for spatial averaging to approach the limit. In the early 1970's, Yuan and Light^{23,24} and coworkers²⁵ developed the theory in terms of path integrals and density matrices. Recently, Ullmo, Baranger, and coworkers^{26,27} studied the nature of quantum oscillations in application to quantum dots.

What is the significance of our results for the real world of 3d, interacting electrons? Our results, for a very different case, reveal the nature of the corrections to local approximations. These will differ in detail depending on the dimensionality of the system, or the specific functional being approximated. However, qualitative features (such as the local approximation becoming exact in the classical continuum limit, gradient expansions being invalid near turning points, etc.) are general. Thus our analysis can (and already has²⁸) provided guidance for the construction of new XC density functionals. On the other hand, there is also a considerable amount of work done in the field of orbital-free DFT,^{29,30} but effort is focused on finding an accurate approximation to the non-interacting kinetic energy as an explicit functional of the density. The present work derives potential functional approximations, an entirely different matter, and so has

no overlap with existing work in that field. Our work suggests that the potential is a better variable than the density, and we show how corrections to local approximations of the density and kinetic energy density can be derived as potential functionals for simple model systems, but the methods and results shown here do not readily generalize to three dimensions.

This paper is divided as follows: In Sec. II, we introduce our notation and define the continuum limit and show that local approximations become exact in this limit. Next, in Sec. III we derive the leading corrections for both the density and kinetic energy density as functionals of the potential by explicit summation of WKB orbitals. Then, in Sec. IV we “fix” the difficulties at the walls to produce a uniform approximation everywhere, and then study its properties comparing to the exact result both in the classical continuum and the large- N limits. Finally, in Sec. V we discuss the implications and relevance for real electronic structure calculations. In the appendix we give a detailed derivation of the interior solution of the density and the KED using the WKB Green’s function in the complex plane, just as has been done before.

II. CLASSICAL CONTINUUM

In this section, we introduce our notation and briefly review the salient points known from the literature. As discussed in the introduction, we restrict ourselves to non-interacting particles in one dimension. We use atomic units throughout ($e^2 = \hbar = m_e = 1$), so that lengths are expressed in Bohr radii, and energies in hartree.

A. Background and notation

We write the Hamiltonian as

$$\hat{h} = \hat{t} + \hat{v} = -\frac{1}{2} \frac{d^2}{dx^2} + v(x), \quad (1)$$

where a hat denotes an operator with \hat{t} being the kinetic energy operator, and $v(x)$ the potential. We denote the solutions to the Schrödinger equation as

$$\hat{h} \phi_j(x) = \epsilon_j \phi_j(x), \quad j = 1, 2, \dots \quad (2)$$

The solutions to the Schrödinger equation can be expanded in powers of \hbar ,³¹ and retaining just the first two, we find the WKB solutions for a given energy ϵ are

$$\phi^{\text{WKB}}(x) = \frac{1}{\sqrt{k(x)}} e^{i\theta(x)}, \quad (3)$$

and its complex conjugate, where the dependence on ϵ is via the definitions of the wavevector

$$k(x) = \sqrt{2(\epsilon - v(x))} \quad (4)$$

and classical phase

$$\theta(x) = \int^x dx' k(x'), \quad (5)$$

where the constant is arbitrary. These solutions are exact when the potential is constant, and highly accurate when the potential is slowly varying on a scale determined by the energy. However, the particular combination that forms an eigenstate depends on the boundary conditions. The density is then

$$n(x) \approx \frac{1}{\pi} \int_{-\infty}^{\mu} d\epsilon |\phi^{\text{WKB}}(\epsilon, x)|^2 = \frac{k_{\mu}(x)}{\pi}, \quad (6)$$

where $k_{\mu}(x)$ is the wavevector evaluated at μ , the chemical potential for the system, found via normalization. Note that $k_{\mu}(x)$ is a function of $\mu - v(x)$ alone, so we define the *local* chemical potential:

$$\mu(x) = \mu - v(x). \quad (7)$$

Then, because WKB is exact for an infinitely extended system with constant potential (free particles), we find

$$n^{\text{unif}}(\mu) = \frac{1}{\pi} (2\mu)^{1/2}, \quad t^{\text{unif}}(\mu) = \frac{1}{6\pi} (2\mu)^{3/2}. \quad (8)$$

The corresponding integrals are local *potential* approximations (LPAs) to the particle number and kinetic energy:

$$\begin{aligned} N^{\text{loc}}[\mu(x)] &= \int dx n^{\text{unif}}(\mu(x)), \\ T^{\text{loc}}[\mu(x)] &= \int dx t^{\text{unif}}(\mu(x)). \end{aligned} \quad (9)$$

Inverting the relation $n^{\text{unif}}[\mu(x)]$ and inserting into $t^{\text{unif}}[\mu(x)]$ yields the local *density* approximation to T :

$$T^{\text{loc}}[n] = \int dx t^{\text{unif}}(n(x)), \quad t^{\text{unif}}(n(x)) = \frac{\pi^2 n^3(x)}{6}. \quad (10)$$

This is the one-dimensional analog of the TF kinetic energy density functional (up to simple factors of 2 for double occupation).³²

One can also work backwards from the LDA to the WKB results. The LDA for the kinetic energy allows us to find an approximate density for a given potential, by minimizing the total energy subject to the constraint of a given particle number. This produces

$$\frac{\pi^2}{2} n^2(x) + v(x) = \mu, \quad (11)$$

the TF equation for this problem, which is identical to Eq. (6). The solution is the TF density, $n^{\text{TF}}(x) = n^{\text{unif}}(\mu(x))$. The total particle number N is a continuous monotonic function of the parameter μ that is invertible for $\mu > v_{\min}$, the minimum of the potential.

The leading corrections to the WKB wavefunctions, i.e., the next two powers in \hbar , are well-known¹⁹ and produce constant corrections to both the phase and the wavevector. Samaj and Percus³² showed very elegantly how the series can be generated to any desired order. Continuing with the higher-order corrections to WKB leads to corrections that depend on derivatives of the potential, where $v'(x) = dv/dx$. The potential gradient expansion for the density is

$$n^{\text{GEA}}[\mu(x)](x) = n^{\text{unif}}(\mu(x)) \left(1 - \frac{v''(x)}{12k_\mu^4(x)} + \frac{v'^2(x)}{8k_\mu^6(x)} + \dots \right), \quad (12)$$

and for the kinetic energy density

$$t^{\text{GEA}}[\mu(x)](x) = t^{\text{unif}}(\mu(x)) \left(1 - \frac{3v''(x)}{4k_\mu^4(x)} + \frac{5v'^2(x)}{8k_\mu^6(x)} + \dots \right), \quad (13)$$

which, when inverted leads to the density *gradient expansion* for T :

$$T[n] \approx \frac{\pi^2}{6} \int dx n^3(x) - \frac{1}{12} \int dx \left[\frac{n'^2(x)}{2n(x)} + n''(x) \right] + \dots \quad (14)$$

A gradient expansion approximation is the finite truncation of that series. Because the semiclassical expansion is asymptotic, this is an asymptotic expansion for periodic systems where μ is above the maximum of the potential. It can be made arbitrarily accurate by application to sufficiently smooth densities, but for any given density, addition of sufficient terms will eventually lead to divergence. For example, a potential that contains steps will produce divergences beyond the lowest order. Also, Coulomb potentials are known to vary too rapidly for such expansions to apply.³³ We note that, in 1d, because of the negative coefficient in the gradient correction, minimizing the total energy is unbounded and nonsensical in the presence of this correction.³⁴ We also note that \hbar never appears in the functional dependence on the density in Eq. (14).

B. The classical continuum limit

We define a continuum as any region of energy in which the eigenvalues of the Hamiltonian are not discrete. The first, simplest example is that of a particle in a well, with a potential set that vanishes as $|x| \rightarrow \infty$. For $\epsilon > 0$, there is the free-particle continuum, with scattering states of the system that cannot be box-normalized. Another continuum arises in solid-state physics, when we apply periodic boundary conditions to our potentials, in order to simulate bulk matter. Then, for single-particle states, the energy levels form distinct bands, usually labelled by a wavevector. Within each band, the energy is continuous. We call this the bulk or thermodynamic continuum.

But any system also has a classical continuum, which can be found by letting $\gamma \rightarrow 0$, where we have replaced \hbar

by $\gamma\hbar$. As γ becomes very small, the discrete levels of the system merge, and the envelope of their density of states approaches a well-defined limit. We call this limit the classical continuum. While it has been long understood that local density approximations become exact in this limit,³⁵ relatively little attention has been paid to how exactly this limit is reached in a quantum system.

Consider a 1d box of length L with given potential $v(x)$ and particle number N , i.e., the lowest N eigenstates are occupied. Then increase the particle number to N' , but

$$\gamma = N/N' \leq 1 \quad (15)$$

i.e., \hbar is reduced in proportion to the increase in particle number. Of course, there will now be N' particles in our well, so define

$$\tilde{n}_\gamma(x) = \frac{N}{N'} n_\gamma(x) \quad (16)$$

as a renormalized density, whose particle number matches the original value at $\gamma = 1$. This process is illustrated in Fig. 2, where we plot renormalized densities for several particle numbers N' , and the TF result in the same potential as used for Fig. 1. One can see

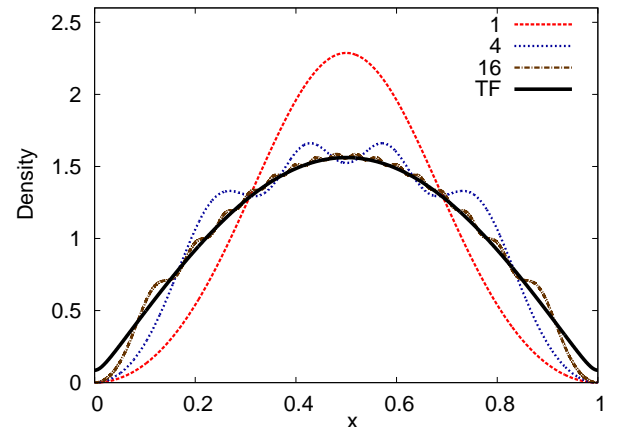


FIG. 2: TF and renormalized exact densities for $N' = 1, 4$, and 16 particles in $v(x) = -12 \sin^2(\pi x)$, $0 \leq x \leq 1$, showing approach to continuum limit.

how our procedure reproduces the TF density, almost. As N' grows, the oscillations in the interior of the box become smaller (with an amplitude of $O(1/N')$), while at the edges (within $O(L/N')$ of the wall), the exact density always drops to satisfy the boundary condition, while the TF density does not. So we also define a moving average of a function of x as:

$$\langle n(x) \rangle_{\Delta x} = \int_{x-\Delta x/2}^{x+\Delta x/2} dx' n(x') / \Delta x. \quad (17)$$

The length scale of the moving average is chosen to be much larger than that of the quantum oscillations of the

exact density and of the boundary region at the wall, but still vanishes as $\gamma \rightarrow 0$. Then, finally,

$$\lim_{\gamma \rightarrow 0} \langle \tilde{n}_{\gamma(N', \mu)}(\mu, x) \rangle_{\sqrt{\gamma}L} = n_N^{\text{TF}}(x). \quad (18)$$

Thus we see that the TF density in a given problem is the limit as $\gamma \rightarrow 0$, but the convergence is highly non-uniform. At the walls, the true density is always zero, but the TF density is finite. There are likely many other averaging procedures, such as taking the limit as a finite temperature vanishes, which can be used to define the limit, but the current one is sufficient for our present purpose. Similarly, we define $\tilde{t}_\gamma(x) \equiv \gamma^3 t_\gamma(x)$.

III. LEADING CORRECTIONS TO LOCAL APPROXIMATIONS

In this section, we derive the leading corrections in γ semiclassically, using only elementary techniques, for the sake of transparency. The first such derivation was by Kohn and Sham,¹⁴ using a very elegant analysis of the properties of the Green's function in the complex plane. We include an appendix in which we also derive our results via this method. In this section, we simply derive formulas for large N and extract the γ -dependence from such formulas.

A. Density

As in Sec. II, the density of N non-interacting fermions is approximated by the sum of the squares of the WKB orbitals, normalized and satisfying the boundary conditions. Because we are deriving the leading corrections, we carefully normalize here:

$$\phi_j^{\text{WKB}}(x) = \sqrt{\frac{2}{k_j(x)T_j}} \sin \theta_j(x), \quad (19)$$

where the normalization constant is found by ignoring the oscillating term. Define

$$\tau_j(x) = \int_0^x \frac{dx}{k_j(x)}, \quad T_j = \tau_j(L), \quad (20)$$

the classical time for a particle in level j to travel from 0 to L . Thus, in WKB theory, the density is approximated by

$$n^{\text{WKB}}(x) = \sum_{j=1}^N \frac{1 - \cos 2\theta_j(x)}{k_j(x)T_j}. \quad (21)$$

Performing the sum exactly yields nothing other than the standard WKB approximation to the density as the sum of WKB densities³⁶. However, such an approximation is inconsistent, since it retains the discrete nature of the eigenvalues, and will not yield a sum with a well-defined

expansion in \hbar . We wish to develop approximations that are smooth in \hbar , and yield the exact approach to the classical continuum limit, ignoring the discrete nature of the eigenstates, i.e., we wish to build in the smooth envelope of functions such as the density. At the end, we requantize our results, and find more accurate summations than WKB, even for $N = 1$.

Begin with the smooth (non-oscillating) contribution. We use the Euler-Maclaurin formula in the following form:

$$\sum_{j=1}^N f_j = \int_{\frac{1}{2}}^{N+\frac{1}{2}} dj f_j - \frac{1}{24}(f'_F - f'_m) + \mathcal{O}(f''), \quad (22)$$

where prime denotes a derivative with respect to j and a subscript F denotes evaluation at the upper limit of the integral, $j_F = N + 1/2$, while a subscript m denotes evaluation at the lower limit, $j = 1/2$. This is an expansion for sums in the same parameter as for the WKB eigenfunctions, i.e., gradients of the potential. We retain only the first two terms, consistent with our WKB approximation for the orbitals.

To expand the sum of the smooth terms in such powers, we need to relate the level index j with the energy in a continuous fashion. Write the WKB quantization condition as

$$\Theta_j = \theta(\tilde{\epsilon}_j, L) = j\pi, \quad j = 1, 2, \dots \quad (23)$$

which defines $\tilde{\epsilon}_j$, the WKB eigenvalue implicitly. Then differentiation yields:

$$\Theta'_j = T_j \tilde{\epsilon}'_j = \pi, \quad (24)$$

where $\mu_{\text{sc}} = \tilde{\epsilon}_F = \tilde{\epsilon}_{N+1/2}$. This allows us to apply Eq. (22) to the smooth contribution from Eq. (21). Define

$$\kappa_j(x) = \frac{1}{k_j(x)T_j}, \quad (25)$$

which has units of inverse length and whose j -dependence is typically weak, vanishing entirely for a flat box. Then

$$\sum_{j=1}^N \kappa_j(x) \approx \int_{\frac{1}{2}}^{N+\frac{1}{2}} dj \kappa_j = \int_{k_m}^{k_F} \frac{dk}{\pi}, \quad (26)$$

where we have neglected terms that contain derivatives of κ_j at the end points. Thus

$$\sum_{j=1}^N \kappa_j(x) \approx (k_F(x) - k_m(x)) / \pi, \quad (27)$$

where the quantities in the integrand of Eq. (26) depend on j in a continuous manner, $k_F(x) = \sqrt{2\mu_{\text{sc}}(x)}$ and μ_{sc} satisfies the quantization condition in Eq. (23) with $j = N + 1/2$, while $k_m(x)$ is the same but with $N = 0$.

The oscillating term in Eq. (21) is more delicate. For each x , we expand $\theta_j(x)$ about its value at the Fermi level linearly

$$\theta_j(x) = \theta_F(x) - (j_F - j) \alpha_F(x) + \dots, \quad (28)$$

where

$$\alpha_j(x) = \theta'_j(x) = \pi \frac{\tau_j(x)}{T_j}. \quad (29)$$

If we truncate at this level, and use the geometric sum defined by

$$h^{(0)}(z) = \sum_{j=1}^N z^j = z \frac{1 - z^N}{1 - z}, \quad (30)$$

and using $z = \exp[i 2\alpha_F(x)]$, we find

$$- \sum_{j=1}^N \frac{\cos 2\theta_j(x)}{k_j(x) T_j} = \frac{k_m(x)}{\pi} - \frac{\kappa_F(x) \sin 2\theta_F(x)}{2 \sin \alpha_F(x)}. \quad (31)$$

The first term here exactly cancels the second term of the smooth contribution in Eq. (27). It is found from performing the geometric sum, using Eq. (28) to undo the linear approximation at the lower end of the sum in Eq. (31). Hence, the semiclassical density is

$$n_{sc}(x) = n_s(x) + n_{osc}(x), \quad (32)$$

where s denotes the smooth term,

$$n_s(x) = \frac{k_F(x)}{\pi}, \quad (33)$$

and osc the oscillating contribution, defined to have zero moving average as $\gamma \rightarrow 0$,

$$n_{osc}(x) = - \frac{\sin 2\theta_F(x)}{2T_F k_F(x) \sin \alpha_F(x)}. \quad (34)$$

Note how completely different these corrections are from those of Eq. (12). This is a central result of this work.

In general, the smooth term does *not* match that of TF theory, because it is evaluated at $N + 1/2$, not N . This is not an artifact of Eq. (22), but reflects the $1/2$ electron loss of density in the quantum correction. We write Eq. (22) in a form that avoids terms with f_m and f_F , but the $1/2$ term is independent of any particular choice.

Note also that our semiclassical density is not normalized, in general. For a flat box, the quantization *does* imply correct normalization, but not more generally. It is straightforward to find slightly modified definitions of $\theta(x)$, etc., that both normalize the density and satisfy the boundary conditions (i.e., $\Theta = j\pi$), but we choose to retain this error as a measure of the error in our semiclassical approximations. We discuss this fact and assess the error in Sec. IV A.

Finally, we can rewrite the result as:

$$n_{sc}(x) = \frac{k_F(x)}{\pi} [1 - \eta(x) f(\alpha_F) w(\theta_F)], \quad (35)$$

where $f(\alpha) = 1/\sin \alpha$, $w = \sin(2\theta)$, and

$$\eta(x) = \frac{\pi}{2k_F^2(x) T_F} = \frac{\hbar \omega_F}{8(\mu_{sc} - v(x))} \quad (36)$$

is the small parameter, once x is not too close to the wall, and $\omega_F = 2\pi/T_F$ is the classical frequency of collisions with the walls at the Fermi energy. To show the γ -dependence explicitly, replace N by N/γ and write

$$\begin{aligned} \tilde{n}_{sc,\gamma}(x) &\equiv \gamma n_{sc, \frac{N}{\gamma}}(x) \\ &= \gamma \left(\frac{k_{F,\gamma}(x)}{\pi} - \frac{\sin 2\theta_{F,\gamma}(x)}{2T_{F,\gamma} k_{F,\gamma}(x) \sin \alpha_{F,\gamma}(x)} \right), \end{aligned} \quad (37)$$

where F, γ denotes evaluation at $N/\gamma + 1/2$.

B. Kinetic energy density

A similar analysis can be applied to the kinetic energy density, but must be done more carefully:

$$t(x) = \sum_{j=1}^N \frac{k_j^2(x)}{2} |\phi_j(x)|^2 \approx \sum_{j=1}^N \frac{\xi_j(x)}{2} (1 - \cos 2\theta_j(x)), \quad (38)$$

where $\xi_j(x) = k_j^2(x) \kappa_j(x)$. First we evaluate the sum over the smooth contribution using the same logic as for the smooth piece of the density. Applying Eq. (22) we obtain

$$\sum_{j=1}^N \frac{\xi_j(x)}{2} \approx \left[\frac{k_j^3}{6\pi} - \frac{\xi'_j}{48} \right]_{\frac{1}{2}}^{N+\frac{1}{2}} + O(\xi''). \quad (39)$$

We know that the contributions from the lower end will be cancelled by analogous contributions in the oscillating piece. To evaluate that, we define:

$$h^{(p)}(z) = \sum_{j=1}^N (j_F - j)^p z^j = z h^{(p-1)'}(z) - j_F h^{(p-1)}(z), \quad (40)$$

where $h^{(p)'}(z) = dh^{(p)}/dz$.

Each term has many terms, but only those containing a z^N will contribute to our answer, because when we insert Eq. (28) into Eq. (38), the prefactor contains z^{-N} . Then

$$t_{osc}(x) = -\frac{1}{2} \Re \left\{ e^{2i(\theta_F - j_F \alpha_F)} \left[\xi_F h^{(0)} - \xi'_F h^{(1)} + \frac{1}{2} \xi''_F h^{(2)} \right]_{z=e^{2i\alpha_F}} \right\}. \quad (41)$$

Evaluating term by term yields

$$t_{osc}(x) = \frac{1}{16} \left\{ \xi_F f \frac{\partial^2 w}{\partial \theta^2} + \xi'_F \frac{\partial f}{\partial \alpha} \frac{\partial w}{\partial \theta} + \frac{1}{2} \xi''_F \frac{\partial^2 f}{\partial \alpha^2} w \right\}. \quad (42)$$

The derivatives of ξ w.r.t. j can be written as

$$\xi'_j = 2\pi\xi_j^2/k_j^3 + k_j^2\kappa'_j \quad (43)$$

and

$$\xi''_j = 2\pi^2\xi_j^3/k_j^6 + 6\pi\kappa'_j/T_j + k_j^2\kappa''_j. \quad (44)$$

We now drop all derivatives of κ_j , because they vanish in the flat box limit, yielding:

$$\tilde{t}_{\text{sc}}(x) = \frac{k_F^3}{6\pi} \left[1 + \frac{3}{4}\eta f \frac{\partial^2 w}{\partial \theta^2} + \eta^2 \left(3 \frac{\partial f}{\partial \alpha} \frac{\partial w}{\partial \theta} - 1 \right) + 3\eta^3 \frac{\partial^2 f}{\partial \alpha^2} w \right]. \quad (45)$$

Again, the explicit γ -dependence of this formula is found by replacing N by $N + 1/2$. As we shall show in later sections, this result is less well-behaved than that for the density. For example, when the potential is non-uniform, the semiclassical kinetic energy density of Eq. (45) incorrectly fails to vanish at the edges.

To overcome this failure, we define the edge as being those values of x up to some fraction β of a period of the classical phase:

$$\theta_F(x_\beta) = \beta\pi, \quad (46)$$

such that the edge region is $x < x_\beta$ and $x > L - x_\beta$. We choose $\beta = 1/4$ (and the interior is all the rest). This mimics the approach used in boundary-layer theory for differential equations, which can be applied to the \hbar -expansion of the individual levels. One constructs approximations that are correct to a given order in the asymptotic expansion in each region separately, and hopes to find a middle region where they match, yielding a solution with uniform convergence properties,¹⁹ i.e., with the correct asymptotic expansion for any x . The only difference here is that we are applying these ideas to the sum of levels, not the individual levels themselves.

Our final semiclassical approximation for the KED is

$$t_{\text{sc}}(x) = \begin{cases} \tilde{t}_{\text{sc}}(x) & \text{if } x_\beta < x < L - x_\beta, \\ \tilde{t}_{\text{sc}}^{\text{unif}}(x) & \text{else,} \end{cases} \quad (47)$$

where

$$\begin{aligned} \tilde{t}_{\text{sc}}^{\text{unif}}(x) = & \frac{(k_F^{\text{unif}})^3}{6\pi} - \frac{(k_F^{\text{unif}})^2 \sin(2k_F^{\text{unif}}x)}{4L \sin(\pi x/L)} \\ & - \frac{\pi k_F^{\text{unif}} \cos(\pi x/L) \cos(2k_F^{\text{unif}}x)}{4L^2 \sin^2(\pi x/L)} \\ & - \frac{\pi^2 \sin(2k_F^{\text{unif}}x)}{8L^3 \sin(\pi x/L)} \left(\frac{1}{2} - \frac{1}{\sin^2(\pi x/L)} \right). \end{aligned} \quad (48)$$

Hence, inside the edge region we approximate the KED by $\tilde{t}_{\text{sc}}^{\text{unif}}(x)$ meaning that we evaluate Eq. (45) with the local Fermi wavevector for a uniform potential, i.e., replacing k_F everywhere by $k_F^{\text{unif}} = \sqrt{2\mu_{\text{sc}}}$ and defining all other quantities based on that. In particular the classical phase and transit time become linear in x , as k_F^{unif} for the uniform system is independent of x . Hence, the

boundary conditions will always be satisfied, no matter what $v(x)$ is. Outside that region, i.e., in the interior of the box ($x_\beta < x < L - x_\beta$), the nonlocal $k_F(x)$ is used. We illustrate our approximations and the exact KED for

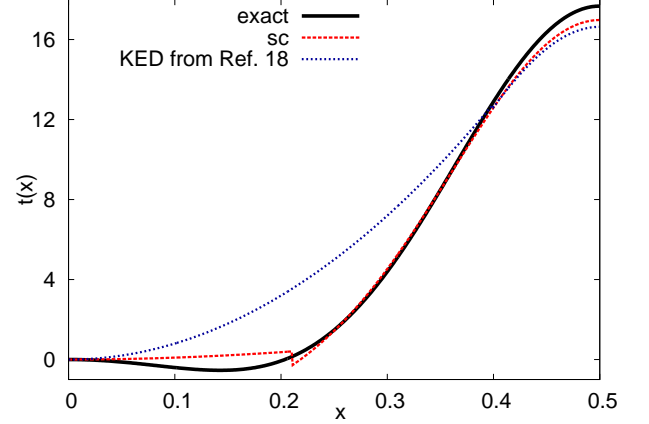


FIG. 3: Exact and approximate ground-state KEDs for $v(x) = -12 \sin^2(\pi x)$, where $0 \leq x \leq 1$. The lowest eigenvalue is $\epsilon_0 = -4.27$ and $\mu_{\text{sc}} = 5.52$.

a single-well potential $v(x) = -12 \sin^2(\pi x)$ within box boundaries in Fig. 3. Note that our present approximation of Eq. (47) is substantially more accurate for both the edge region and the interior than the previously derived KED of Ref. 18. In the next section we discuss this fact more quantitatively.

IV. PROPERTIES

We next test our approximations, to demonstrate both their accuracy and that they have the properties claimed for them. We begin with several integrated quantities, mostly energies.

A. Energies and normalization

The LPA yields densities that are local in the potential, with the exception of the value of the chemical potential, which must be determined globally. The quantum corrections depend on several other terms, such as $\theta_F(x)$ and T_F , which are still simple functionals of the potential, but distinctly non-local, depending on integrals over $v(x)$. To test the integrated properties of the density, we calculate moments over that density. The obvious one is the third moment, as that is simply related to the local *density* approximation to T , evaluated on that density.

We choose a standard potential, $v(x) = -10 \sin^2 \pi x$ in a box of length 1, and insert one particle. Both exact and approximate results are given in Table I.

First note that the TF result, T^{TF} , is about 50% too small, compared to the exact answer, T . This is the result

TABLE I: Exact and approximate quantities for one particle in a single-well potential $v(x) = -10 \sin^2(\pi x)$, $0 \leq x \leq 1$. T is the exact kinetic energy and n the exact density.

Energy levels	ϵ_1	ϵ_2	μ	μ_{sc}
	-2.71	14.6	0.637	6.38
Kinetic energy	T		$T^{\text{loc}}[n]$	
	exact	sc	TF	exact
	5.07	5.02	2.31	4.93
				5.07

of minimizing the energy using LDA as in the first term of Eq. (14).

We measure the quality of the TF density and our semiclassical density by evaluating the LDA kinetic energy on those densities, i.e., $T^{\text{loc}}[n^{\text{TF}}] = T^{\text{TF}}$ and $T^{\text{loc}}[n_{sc}]$, where the point of reference is the LDA kinetic energy evaluated on the exact density, $T^{\text{loc}}[n]$. But the TF result remains about 50% too small compared to $T^{\text{loc}}[n]$. However, the LDA on our semiclassical density, $T^{\text{loc}}[n_{sc}]$, yields an energy only 3% too large, i.e., reducing the error by about a factor of 20.

To test our semiclassical kinetic energy, T_{sc} , we compare with the exact value, T , and find an error of only 0.9% too small, i.e., 50 times better than T^{TF} . Thus the semiclassical results are more than an order of magnitude better than bare DFT results, because they include quantum oscillations. In fact, the LDA kinetic energy evaluated on the exact density, $T^{\text{loc}}[n]$, yields only a 2.7% underestimate, showing that local approximations do much better on accurate densities, but still not as well as our direct approximation, T_{sc} .

These systems do not appear to be particularly *semi-classical*: the potential is not flat nor is the particle number or index high. We can analyze the source of this accuracy by expanding integrated quantities in powers of γ about 0:

$$T(\gamma) = T^{(0)} + \gamma T^{(1)} + \gamma^2 T^{(2)} + \dots \quad (49)$$

For the kinetic energy, from the previous discussion:

$$T^{(0)} = T^{\text{TF}} \quad (50)$$

while our derivation should yield:

$$T^{(1)} = T_{sc}^{(1)}. \quad (51)$$

These results should hold for *both* the local approximation applied to the exact density (and so test our semiclassical density) and the exact kinetic energy (and so test our semiclassical kinetic energy density). In Fig. 4, we study the γ -dependence of $T^{\text{loc}}[n]$ applied to various densities for a generic well. Clearly TF gives the $\gamma = 0$ value, while the semiclassical density includes the correct linear contribution, and is quite accurate for higher-order contributions. We also note that inclusion of the linear term greatly improves over the TF result, but that the LDA kinetic energy evaluated on our semiclassical density is even more accurate still.

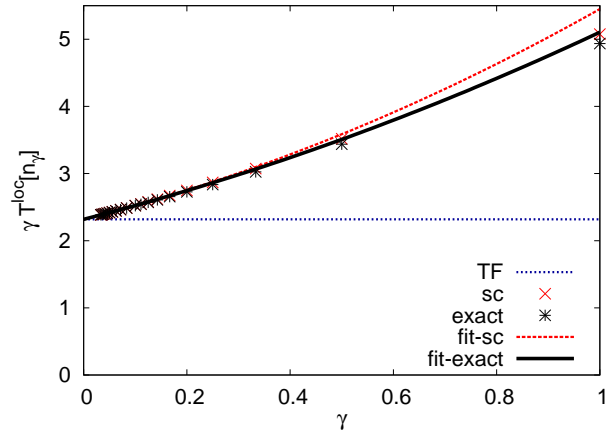


FIG. 4: LDA kinetic energy multiplied by the scale factor γ for different γ evaluated on $n_{\gamma}^{\text{TF}}(x)$, our semiclassical density $n_{sc,\gamma}(x)$, and the exact density for a single-well potential $v(x) = -10 \sin^2(\pi x)$.

Because our expansion is in powers of \hbar , we expect that it is asymptotic, just as the WKB expansion is.¹⁹ Thus, for fixed N and γ , inclusion of additional coefficients in the expansion will eventually *worsen* the result. We can see this in Table II, where the error of our semiclassical result, $|T_{sc} - T|$, at $\gamma = 1$ is smaller than the error in the quadratic coefficients, $|T_{sc}^{(2)} - T^{(2)}|$, and thus cannot be explained in terms of its approximation to that (or any higher) coefficient. On the other hand, the asymp-

TABLE II: Coefficients of γ -expansion in Eq. (49) of the exact and semiclassical kinetic energy, $T^{(i)}$ and $T_{sc}^{(i)}$, and the values T and T_{sc} at $\gamma = 1$ for $v(x) = -10 \sin^2(\pi x)$, where $0 \leq x \leq 1$.

N	$T^{(0)}$	$T^{(1)}$	$T^{(2)}$	$T_{sc}^{(2)}$	T	T_{sc}
1	2.31	2.05	0.614	0.900	5.07	5.02
2	13.4	9.78	1.69	1.62	24.9	24.7

totic expansion with just the first few terms in Eq. (49) becomes accurate very rapidly as N increases. Compare the relative error of the quadratic coefficients of about 50% for $N = 1$ with roughly 4% for $N = 2$. The error dropped by about an order of magnitude as the number of particles increases by one. To understand why that is so, we next consider the N -dependence of each contribution, where N is now the number of particles at $\gamma = 1$. As $N \rightarrow \infty$, the box must appear flat. Evaluating the local approximation on the flat box density yields:

$$T_{\gamma}^{\text{loc}}[n] = \frac{\pi^2 N^3}{6L^2} \left[1 + \frac{9}{8} \left(\frac{\gamma}{N} \right) + \frac{3}{8} \left(\frac{\gamma}{N} \right)^2 \right], \quad (\text{flat}) \quad (52)$$

fixing the first three coefficients with the values above, and the rest to vanish. The corrections to this flat limit can only involve powers of $1/N$, which we can either derive or find numerically.

Since the leading term is given by TF theory, if we expand the potential in the box in a power series around its average value, we find

$$T^{\text{TF}} = \frac{\pi^2 N^3}{6L^2} \left(1 + \frac{3\overline{\delta v^2}}{(\pi\bar{n})^4} + \dots \right) \quad (53)$$

where $\bar{n} = N/L$ and

$$\overline{\delta v^2} = \int_0^L dx (v(x) - \bar{v})^2 / L \quad (54)$$

with \bar{v} the average of the potential over the well. For our shape, $\overline{\delta v^2} = D/8$, yielding a TF value of 2.31, as in the figure. More importantly, we see that the leading correction to the flat box result is $O(1/N^4)$. Similarly, we find by fitting, that

$$T^{(1)} = \frac{3\pi^2 N^2}{16L^2} \left(1 + \frac{a}{N^2} + \frac{b}{N^4} + \dots \right) \quad (55)$$

and is given exactly by the semiclassical approximation. For the specific choice of potential $v(x) = -10 \sin^2(\pi x)$ the coefficients are $a = 0.38$ and $b = -0.26$. Finally,

$$T^{(2)} = \frac{\pi^2 N^2}{16L^2} \left(1 + \frac{c}{N^4} + \dots \right), \quad (56)$$

but the coefficient c is *not* given correctly by the semiclassical approximation. For $v(x) = -10 \sin^2(\pi x)$ the exact value is $c = 0.42$, whereas the semiclassical approximation gives about half that value. Thus, all corrections to the flat results vanish rapidly as N increases, and the errors of the first few semiclassical terms in the expansion become much smaller, leading to a much more accurate value at $\gamma = 1$.

TABLE III: Local approximation to the kinetic energy evaluated on the TF, semiclassical, and exact density, and the kinetic energy from direct integration of the semiclassical and exact KED, all relative to the flat box value for N particles in a single-well potential $v(x) = -10 \sin^2 \pi x$, $0 \leq x \leq 1$. The errors of our semiclassical result with respect to the exact result are denoted by Δsc .

N	$\Delta T^{\text{loc}}[n]$				ΔT		
	TF	sc	exact	Δsc	sc	exact	Δsc
1	-1.8	0.96	0.82	0.14	0.09	0.13	-0.04
2	-8.3	0.89	0.92	-0.03	0.08	0.24	-0.16
4	-32	0.77	0.78	-0.01	0.09	0.14	-0.05
6	-70	0.72	0.73	-0.01	0.07	0.09	-0.02
8	-123	0.70	0.70	0.00	0.06	0.07	-0.01

In Table III, we list the various kinetic energies as functions of N for our well. Because the errors vanish so rapidly, we subtract the energies of the uniform system, as in:

$$\Delta T = T - T^{\text{unif}} \quad (57)$$

and likewise for $\Delta T^{\text{loc}}[n]$. These differences could also be thought of as the change in energy due to turning on the well in the bottom of the box, analogous to the change in energy when atoms form a molecule. We see that our approximations become very accurate very quickly, and converge as $1/N^2$.

The quantum correction yields a density that is *not* normalized. This is because the requirement in Eq. (23) that the phase vanishes at both $x = 0$ and at $x = L$ is used to determine μ_{sc} , not simple normalization. Of course, the error vanishes rapidly as $N \rightarrow \infty$; for $N = 1$, it is $\Delta N = 4 \times 10^{-2}$ and for $N = 2$, $\Delta N = 6 \times 10^{-4}$. One can easily imagine schemes that patch this failure up, but we prefer to leave it as a measure of the overall error in the approximation.

Since our formulas reduce to the exact results for a uniform potential, more generally, they should preserve these good features for a slowly-varying potential. We have applied our density formula to many examples, and *almost always* found it to be remarkably accurate. This is because of its excellent formal properties, and because we capture the leading correction to the LPA in a well-defined (albeit asymptotic) series. Most importantly, it appears that the conditions of application, μ_{sc} above v everywhere, imply that these leading corrections *always* improve over the dominant contribution.

B. Uniform convergence

While the most important aspect of our work is the recovery of the leading asymptotic corrections to TF for the energies, the detailed spatial dependence is also important for understanding how this is achieved, and also for understanding the strengths and weaknesses of this approach.

Our semiclassical approximations are exact in the case of a uniform potential, where they yield the simple formulas:

$$n_{\gamma}^{\text{unif}}(x) = \tilde{N} \left(1 - \frac{\sin(2\pi\tilde{N}x)}{2\tilde{N}\sin\pi x} \right) \quad (58)$$

and Eq. (45) with $f = 1/\sin(\pi x)$, $w = \sin(2\pi\tilde{N}x)$, and $\tilde{N} = (N/\gamma + 1/2)$. These offer some insight into the nature of the expansion.

Consider first the density. For any finite value of x , the oscillating contribution shrinks and oscillates more rapidly as $\tilde{N} \rightarrow \infty$. Thus, we can expand the smooth part, the prefactor of the oscillating contribution, and the phase of the oscillation, in powers of $1/\tilde{N}$, which is linear in γ for small γ . On the other hand, for $\tilde{N}x$ fixed, one can again expand the density for large \tilde{N} :

$$n_{\gamma}(y) = \tilde{N} \left[\left(1 - \frac{\sin 2\pi y}{2\pi y} \right) - \frac{\pi y \sin(2\pi y)}{12\tilde{N}^2} + \dots \right], \quad (59)$$

where $y = \tilde{N}x$. The first term is precisely the profile of a semi-infinite box at the surface. This series is very ill-

behaved for large y , except for the lowest-order term. Similar comments apply to the kinetic energy density only more so, as several contributions *diverge* for small $\tilde{N}x$. Thus there are two distinct regions and limits within the well, the interior and the edges.

In what follows we illustrate that the error of our semiclassical approximations converges uniformly as $\gamma \rightarrow 0$. We define:

$$\Delta n_{\text{sc}}(x) = n_{\text{sc}}(x) - n(x) \quad (60)$$

as the error in the semiclassical density, and likewise for the kinetic energy density. We pick a generic single-well

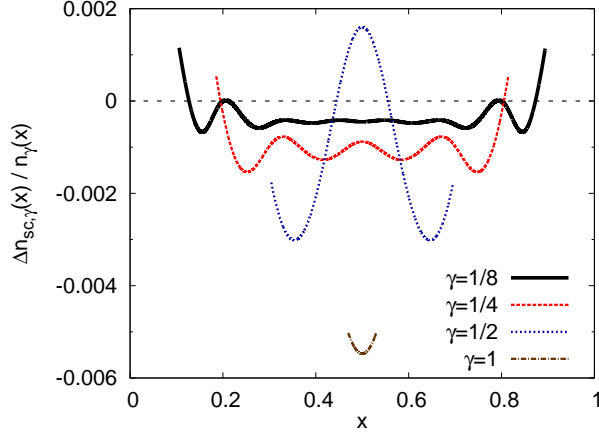


FIG. 5: Fractional error in density for $v(x) = -5 \sin^2(\pi x)$; only shown in interior ($\theta_F/\pi \geq 0.7$ in left half).

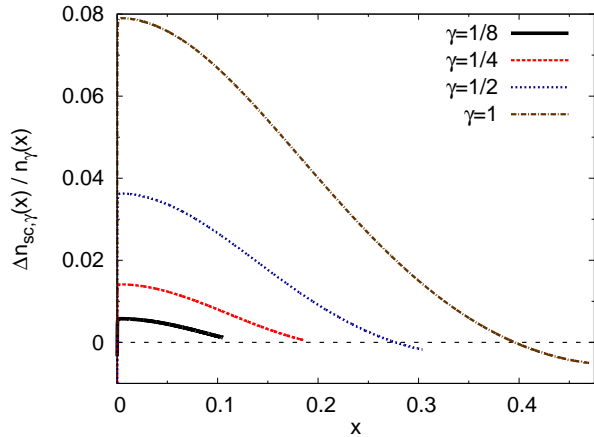


FIG. 6: Fractional error in density close to the edge for $v(x) = -5 \sin^2(\pi x)$, $\theta_F/\pi \leq 0.7$.

potential $v(x) = -5 \sin^2(\pi x)$ sufficiently close to flat so that we are in a regime dominated by the asymptotic behavior. For illustrative purposes we increase the extend of the edge-region by choosing $\beta = 0.7$. The fractional

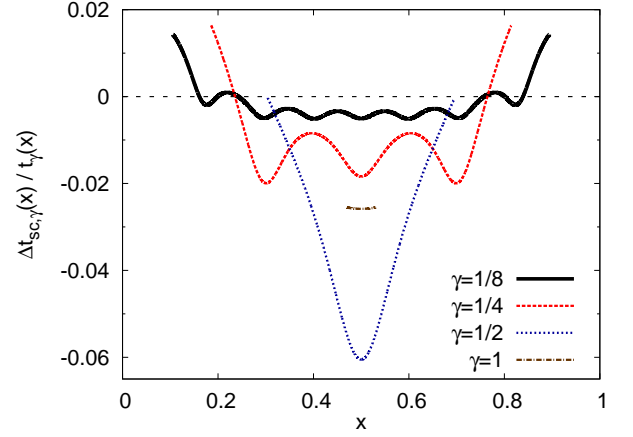


FIG. 7: Same as Fig. 5, for kinetic energy density.

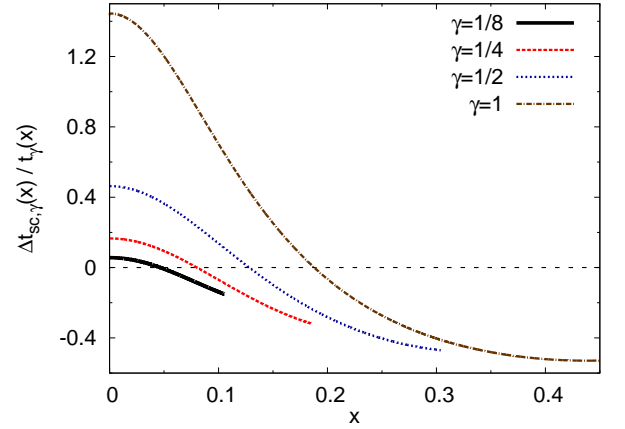


FIG. 8: Same as Fig. 6, for kinetic energy density.

error of the density in the interior is shown in Fig. 5. The error converges uniformly throughout the interior as $\gamma \rightarrow 0$, being $\mathcal{O}(\gamma)$. As shown in Fig. 6, the fractional error close to the edge of the box also converges uniformly, being $\mathcal{O}(\gamma)$ but noticeably larger. The convergence for the KED is shown in Figs. 7 and 8, and has the same features as the density, but is much larger.

C. Phase oscillations

We also check that the quantum oscillations of our semiclassical formulas can be extracted from the exact results as $\gamma \rightarrow 0$. For a fixed point x we look at the difference between the exact result and the smooth term, multiplied by the prefactor appearing in our formula for the quantum oscillations:

$$d_\gamma(x) = 2T_F k_F(x) \sin \alpha(x) \Delta n_{\text{s}, \gamma}(x). \quad (61)$$

If our results are correct, as $\gamma \rightarrow 0$, this becomes a simple function of $S_F(x)/\gamma$, for *any* values of x and γ , specifically $-\sin(2S_F(x)/\gamma)$. The same analysis applies to the kinetic

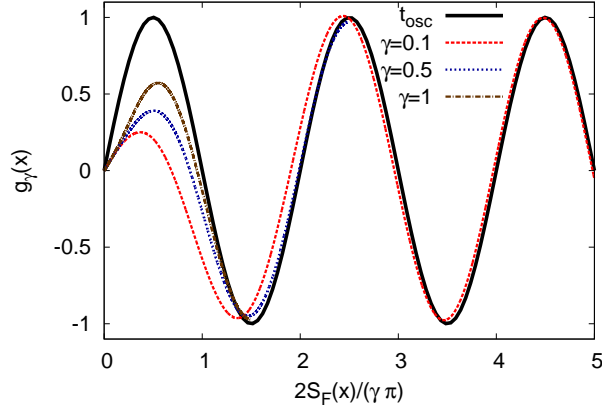


FIG. 9: Leading correction to the kinetic energy density for $\gamma = 1, 0.5, 0.1$ and $v(x) = -10 \sin^2(\pi x)$.

energy density, where we define:

$$g_\gamma(x) = \frac{4T_F \sin \alpha(x)}{k_F(x)} \Delta t_\gamma^{\text{TF}}, \quad (62)$$

In Fig. 9, we plot $g_\gamma(x)$ for several values of γ , as a function of $2\theta_F(x)/\pi$, finding results converging to $-\sin 2\theta_F(x)$, as predicted by the leading term of Eq. (42).

D. Evanescent regions

The only condition on the applicability of our approximations is that $\mu_{\text{sc}} > v(x)$ for all x . But μ_{sc} is between the highest occupied and lowest unoccupied level, and so for many well-depths, it can be the case that the HOMO has turning points while the condition is still valid. The starkest example is for $N = 1$, since beyond those turning points, the only occupied orbital is evanescent. Yet our approximations can still be applied, even though they contain only trigonometric functions of the phase, and no decaying exponentials, and still yield *highly accurate* results. In Figs. 1 and 3 we show results for a well depth of 12, for which the lowest eigenvalue is $\epsilon_0 = -4.27$ and $\mu_{\text{sc}} = 5.52$, and the turning points are located at around $x = 0.2$ and $x = 0.8$. Eventually the quadratic approach of the semiclassical density near the wall of the box mimics the exponential decay of the true density. Even the KED truncated by our method, only misses the negative contribution, which largely cancels the error in the interior. The results for this well remain remarkably accurate. As the semiclassical chemical potential μ_{sc} approaches v_{max} the validity of our approximation breaks down. We simulate such a situation in Figs. 10 and 11 by choosing a well depth of 27, such that μ_{sc} is only slightly

above v_{max} . This is the worst qualitative breakdown of

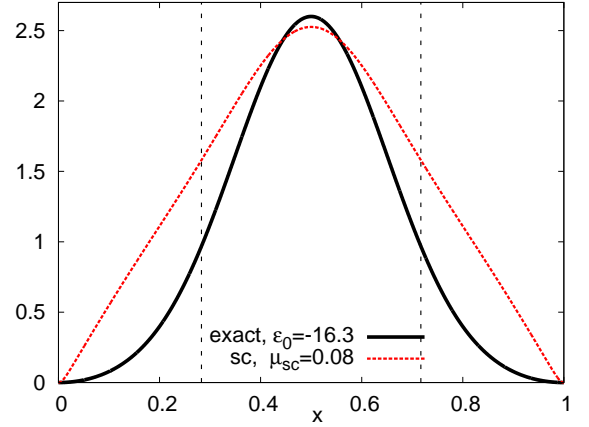


FIG. 10: Exact and approximate ground-state densities for $v(x) = -27 \sin^2(\pi x)$, where $0 \leq x \leq 1$. The lowest eigenvalue is $\epsilon_0 = -16.3$ and $\mu_{\text{sc}} = 0.08$. The position of the turning points is indicated by dashed lines.

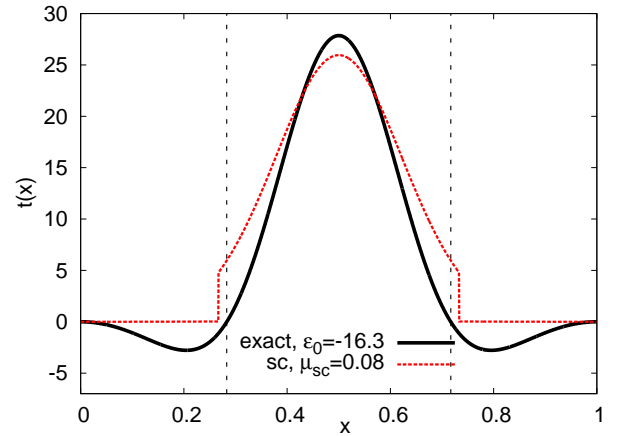


FIG. 11: Exact and approximate ground-state KEDs for $v(x) = -27 \sin^2(\pi x)$, where $0 \leq x \leq 1$. The lowest eigenvalue is $\epsilon_0 = -16.3$ and $\mu_{\text{sc}} = 0.08$. The position of the turning points is indicated by dashed lines.

our approximation, yielding the errors shown in Tab. IV. But even here, errors are $\leq 20\%$.

V. CONSEQUENCES FOR DENSITY FUNCTIONAL THEORY

This work has been confined to one-dimensional non-interacting particles confined by hard walls. In this section, we discuss in detail the ramifications for density functional theory in the real world of atoms, molecules,

TABLE IV: Exact and approximate quantities for one particle in a single well $v(x) = -D \sin^2(\pi x)$, where $0 \leq x \leq 1$.

Energy levels	ϵ_1	ϵ_2	μ	μ_{sc}	
$D = 12$	-4.27	13.6	0.04	5.52	
$D = 27$	-16.3	5.47	-6.75	0.08	
Kinetic energy	T		$T^{\text{loc}}[n]$		
	exact	sc	TF	exact	sc
$D = 12$	5.13	5.18	2.66	5.12	5.33
$D = 27$	5.74	7.63	4.80	6.42	8.47

and solids. We divide the discussion in two: Thomas-Fermi theory and Kohn-Sham theory.

We begin with Thomas-Fermi theory and its extensions. This was the original density functional theory (DFT) and continues to be used in many fields of physics. TF theory became obsolescent for electronic structure calculations with Kohn-Sham work, but there has been a recent resurgence of interest in orbital-free DFT, with the hope of treating systems of much greater size than is presently possible with Kohn-Sham calculations. To do this, all that is needed is an accurate approximation to the non-interacting kinetic energy as a functional of the density. The original approximation using uniform gas inputs, is simply the 3D analog of our 1D local approximation used here. Thus if our methods could be generalized to apply to the general 3D case, it would produce an orbital-free theory.

Perhaps the most important result of this study is to highlight an alternative path. Instead of trying to find *density* functional approximations, we have derived the leading corrections in terms of the *potential*, a perfectly valid alternative variable to the density.³⁷ If general formulas (or algorithms) could be found for finding accurate approximations to $n[v_s](\mathbf{r})$ and $t_s[v_s](\mathbf{r})$, where the subscript s denotes non-interacting, one could use them to avoid solving the Kohn-Sham equations and evaluating any orbitals. At each step in the iteration, one finds $v_s(\mathbf{r})$, the Kohn-Sham potential, using some standard XC functional, and uses this to generate a new density. When self-consistency is reached, the kinetic energy is evaluated and the many-body energy is found in the usual way. A recent study³⁸ shows that this procedure is correct once both approximations are derived from the same approximate Green's function, as ours have been.

Even before such generalizations have been found, we have been able to use results here to deduce information on the 3D kinetic energy functional. In 1d, our results show that the leading corrections to the asymptotic expansion of the kinetic energy in powers of $1/N$ are *not* determined by the gradient expansion for any finite system, but instead are given by the quantum corrections producing quantum oscillations. Ref. 39 is a careful study of the asymptotic expansion for the 3D kinetic energy, and showed how generalizing the gradient expansion to ensure recovery of the asymptotic expansion greatly improved total energies over the gradient expansion, but worsened

other energies, such as those of jellium surfaces. This reflects the difficulty in attempting to capture different physical limits with simple density-functional approximations. Even our simple results cannot be easily encoded in a density functional approximation, but are both simple and (relatively) physically transparent as *potential* functionals.

Almost all modern electronic structure calculations are performed within the Kohn-Sham formalism, which provides a set of self-consistent non-interacting single-particle equations which reproduce the exact single-particle density of the interacting system. In these, the non-interacting kinetic energy is treated exactly, and only a small contribution to the total energy, the XC energy, is approximated as a functional of the density. This contribution is determined by the Coulomb repulsion, and so is a many-body effect.

So, do we learn anything from studying our little toy problems? The answer is definitely yes. Our toy is perhaps the simplest possible system in which one can meaningfully approximate a Schrödinger equation with its density functional analog, and make a local density approximation. So we learn in what limits this becomes relatively exact, and how to find the leading corrections. We learn the nature of these corrections (asymptotic) and how there are multiple length scales in the system. While the details of these lessons depend on the functional we are approximating, some general features of functionals and their approximations can be guessed at, and highly useful analogies can be made.

For example, there are many ways to understand why Kohn-Sham calculations are far more accurate than Thomas-Fermi type calculations, and our analysis produces one more. A KS calculation, by virtue of its orbitals, produces an incredibly accurate density, and we have seen how local-type approximations are much more powerful on accurate densities than on self-consistent densities. Thus not only does a Kohn-Sham calculation approximate only a small fraction of the total energy (the XC piece), but even that part is much more accurately given by a local approximation by virtue of the accurate density.

The insight based on the semiclassical analysis of functionals has already led to significant development in the Kohn-Sham XC functional. Schwinger demonstrated^{40,41} that LDA exchange becomes relatively exact for large Z neutrals. Analysis of the large- Z behavior of modern exchange GGAs^{42,43} shows that the most popular functionals all recover (to within about 20%) the leading corrections to the LDA asymptotic behavior of exchange for atoms. On the other hand, the gradient expansion approximation, based on the slowly-varying limit, does not, being too small by almost exactly a factor of 2. This is entirely analogous to our problem, in which the local approximation recovers the exact dominant term, and a decent approximation to the next correction, but the gradient expansion worsens that agreement. Since such functionals are tested on exchange energy of atoms, and

these cannot be accurate without accurate asymptotic values, this is vital for recovering accurate thermochemistry, which requires accurate atomic energies. On the other hand, bond lengths depend only on small variations in the energy when the bond distances is varied slightly around its equilibrium value, and so do not require accurate energies of isolated atoms. These can be improved upon over regular GGAs by restoring the true gradient expansion and ignoring the asymptotic limit. The recent PBEsol functional²⁸ does exactly this for exchange and produces better lattice parameters for many solids.

VI. SUMMARY

We have presented a fuller and more precise account of the results originally shown in Ref. 18. Kohn and Sham¹⁴ produced asymptotic expansions for the interior, exterior, and turning point regions of the density. In Ref. 18, we presented a uniform approximation for the interior region, but only an asymptotic approximation for the kinetic energy density. Here, by analyzing the breakdown of the method for the boundary regions, we have produced a (nearly) uniform approximation to the kinetic energy.

This work was supported by NSF under grant number CHE-0809859. We also acknowledge support from the KITP under grant number PHY05-51164.

Appendix A: Derivation of the semiclassical density and kinetic energy density in the complex plane

The semiclassical corrections were derived from a contour integral over the semiclassical Green's function in Ref. 18, and we give a fuller account here. The method is well-described in Ref. 14 but we go beyond the aims there, since we require our solution to be uniformly asymptotic, not just producing the correct asymptotic expansion in the interior and we extract also the kinetic energy density. We are also treating box boundary conditions, rather than the turning points discussed there. Begin with the diagonal Green's function

$$g(x, \epsilon) = \frac{2 \phi_L(x) \phi_R(x)}{W(\epsilon)}, \quad (\text{A1})$$

where $W(\epsilon) = \phi_L(x) \partial \phi_R(x) / \partial x - \phi_R(x) \partial \phi_L(x) / \partial x$ is the Wronskian, and approximate the two independent solutions $\phi_L(x)$ and $\phi_R(x)$ via the WKB wavefunctions satisfying the boundary conditions:

$$\phi_L^{\text{WKB}}(x) = \sin[\theta(x)] / \sqrt{k(x)}, \quad (\text{A2})$$

$$\phi_R^{\text{WKB}}(x) = \sin[\theta(L - x)] / \sqrt{k(x)}, \quad (\text{A3})$$

yielding

$$g_{\text{sc}}(x, \epsilon) = \frac{\cos \Theta - \cos [2\theta(x) - \Theta]}{k(x) \sin \Theta} = g_s(x, \epsilon) + g_{\text{osc}}(x, \epsilon). \quad (\text{A4})$$

Thus,

$$n_{\text{sc}}(x) = \oint_{C(\mu_{\text{sc}})} \frac{d\epsilon}{2\pi i} g_{\text{sc}}(x, \epsilon) = n_s(x) + n_{\text{osc}}(x), \quad (\text{A5})$$

where $C(\mu_{\text{sc}})$ is a contour enclosing all poles of occupied states determined by μ_{sc} .

First we evaluate the density coming from the smooth term. In the limit $L \rightarrow \infty$ this is dominated by $\exp[-i\Theta]$, simplifying the integral to

$$n_s(x) = -\frac{1}{2\pi} \oint_{C(\mu_{\text{sc}})} \frac{d\epsilon}{k(x, \epsilon)}, \quad (\text{A6})$$

which, evaluated on the real axis, yields:

$$n_s(x) = \frac{1}{\pi} \int_{v(x)}^{\mu_{\text{sc}}} \frac{d\epsilon}{k(x, \epsilon)} = \frac{k_F(x)}{\pi}. \quad (\text{A7})$$

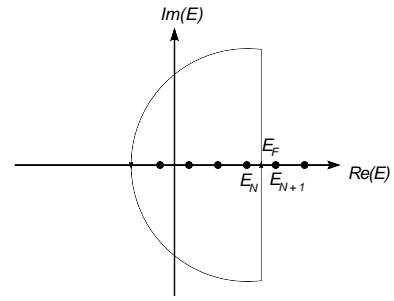


FIG. 12: Contour of integration in the complex ϵ -plane.

Then, we evaluate the oscillating term of Eq. (A4). We pick a contour $C(\mu_{\text{sc}})$ as shown in Fig. 12, i.e., a vertical line along $\epsilon = \mu_{\text{sc}} + i\zeta$ connected to a semi-circle, which encloses all poles of N lower-lying energy-eigenvalues $\epsilon_N, \dots, \epsilon_1$. In the classical continuum limit $\mu_{\text{sc}} \gg \zeta$, allowing us to expand all quantities in the integrand in powers of the imaginary part of the energy, ζ :

$$\frac{1}{k(\mu_{\text{sc}} + i\zeta, x)} = \frac{1}{k_F(x)} \left(1 - \frac{i\zeta}{k_F^2(x)} + \dots \right), \quad (\text{A8})$$

$$\theta(\mu_{\text{sc}} + i\zeta, x) = \theta_F(x) + i\zeta \tau_F(x) + \dots \quad (\text{A9})$$

Keeping terms up to first order in ζ , employing the semiclassical quantization condition for the given boundary conditions in Eq. (23) with $j = N + 1/2$, and substituting $u = 4T_F \zeta$, we obtain the result in Eq. (35). Note that the additional term of $1/2$ in the quantization condition relative to Ref. 14 is due to the Mazlov index for a hard wall being 0, rather than $1/4$ at a real turning point.

Next, we provide some details of the lengthy derivation of the kinetic energy density of non-interacting, same-spin fermions:

$$t_{\text{sc}}(x) = \oint_{C(\mu_{\text{sc}})} \frac{d\epsilon}{2\pi i} [\epsilon - v(x)] g_{\text{sc}}(x, \epsilon) = t_s(x) + t_{\text{osc}}(x). \quad (\text{A10})$$

In analogy to the derivation of the semiclassical density we first evaluate the smooth term yielding

$$t_s^{(1)}(x) = \frac{k_F^3(x)}{6\pi}. \quad (\text{A11})$$

The subdominant piece of smooth term gives another contribution:

$$t_s^{(2)}(x) = \oint_{C(\mu_{sc})} \frac{d\epsilon}{2\pi i} \frac{k(x, \epsilon) \exp i\Theta(\epsilon)}{4 \sin \Theta(\epsilon)} \quad (\text{A12})$$

is evaluated on the contour $C(\mu_{sc})$ as shown in Fig. 12. Hence, all quantities in the integrand are expanded in powers of ζ . In particular, we define $s = -2i\Gamma(\zeta)$, where $\Gamma(\zeta) = \int_0^L dx [\sqrt{2[\mu_{sc}(x) + i\zeta]} - \sqrt{2\mu_{sc}(x)}]$, express the ζ -expansion of all quantities in terms of $s(\zeta)$, and truncate its expansion after the quadratic term. Note that we approximate terms like $[\int_0^L dx k_F^3(x)]/T_F$ by $1/k_F^2(x)$. This amounts to the same as neglecting the derivatives of κ_j . Then we obtain

$$t_s^{(2)}(x) = \frac{1}{2\pi k_F(x) T_F^2} \int_0^\infty ds \frac{sz}{z - e^s}, \quad (\text{A13})$$

where $z = \exp[2i\Theta_F]$, which yields

$$t_s^{(2)}(x) = -\frac{\pi}{24k_F(x) T_F^2}, \quad (\text{A14})$$

where the total contribution of the smooth term is the sum of $t_s^{(1)}$ and $t_s^{(2)}$, agreement with Eq. (39). Then, we evaluate the oscillating term, which is integrated also along the contour $C(\mu_{sc})$ in Fig. 12.

We write the cosine of the oscillating piece as a weighted sum of exponential functions and demonstrate the derivation for the term that has the positive sign in the exponential function. We call this term $t_{osc}^{(1)}$.

As before we expand all quantities in powers of ζ . Here, we define $q = -4i\Gamma(\zeta)$, express the ζ -expansion of all quantities in the integrand by $q(\zeta)$, and truncate its expansion after the quadratic term. Then we integrate by aid of the polygamma functions of order n ,⁴⁴ defined as $\psi^{(n)}(l) = (-1)^{n+1} \int_0^\infty dq q^n \exp(-lq)/[1 - \exp(-q)]$, yielding

$$\begin{aligned} t_{osc}^{(1)}(x) = & -\frac{k_F(x)}{8\pi T_F} \left[\psi\left(\frac{y+1}{2}\right) - \psi\left(\frac{y}{2}\right) \right] \sin 2\theta_F(x) \\ & - \frac{1}{16\pi k_F(x) T_F^2} \left[\psi^{(1)}\left(\frac{y}{2}\right) - \psi^{(1)}\left(\frac{y+1}{2}\right) \right] \cos 2\theta_F(x) \\ & - \frac{1}{128\pi T_F^3 k_F^3(x)} \left[\psi^{(2)}\left(\frac{y+1}{2}\right) - \psi^{(2)}\left(\frac{y}{2}\right) \right] \sin 2\theta_F(x) \end{aligned} \quad (\text{A15})$$

Similarly, the other term $t_{osc}^{(2)}$ integrates to the result in Eq. (A15) with $y \rightarrow -y + 1$, where $y = \alpha_F(x)/\pi$. The particular combination of the polygamma functions in $t_{osc}^{(1)}$ and $t_{osc}^{(2)}$ yields

$$\begin{aligned} t_{osc}(x) = & -\frac{k_F(x) \sin 2\theta_F(x)}{4T_F \sin \alpha_F(x)} - \frac{\pi \cos \alpha_F(x) \cos 2\theta_F(x)}{4k_F(x) T_F^2 \sin^2 \alpha_F(x)} \\ & - \frac{\pi^2 \sin 2\theta_F(x)}{8T_F^3 k_F^3(x) \sin \alpha_F(x)} \left(\frac{1}{2} - \frac{1}{\sin^2 \alpha_F(x)} \right). \end{aligned} \quad (\text{A16})$$

Finally, the sum of the smooth and oscillating pieces yield the result of Eq. (45).

-
- ¹ *The Calculation of Atomic Fields*, L.H. Thomas, Proc. Camb. Phil. Soc. **23**, 542 (1927).
 - ² *A statistical method for the determination of some atomic properties and the application of this method to the theory of the periodic system of elements*, E. Fermi, Zeit. f. Physik **48**, 73 (1928).
 - ³ *On the Stability of Molecules in the Thomas-Fermi Theory*, E. Teller, Rev. Mod. Phys. **34**, 627 (1962).
 - ⁴ *A Simplification of the Hartree-Fock Method*, J.C. Slater, Phys. Rev. **81**, 385 (1951); *A Generalized Self-Consistent Field Method*, ibid. **91**, 528 (1953).
 - ⁵ *Inhomogeneous Electron Gas*, P. Hohenberg and W. Kohn, Phys. Rev. **136**, B 864 (1964).
 - ⁶ *Self-consistent Equations Including Exchange and Correlation Effects*, W. Kohn and L.J. Sham, Phys. Rev. **140**, A 1133 (1965).
 - ⁷ R.M. Martin, *Electronic Structure, Basic Theory and Practical Methods* (Cambridge University Press, Cambridge, 2004).
 - ⁸ *Which functional should I choose?*, D. Rappoport, N.R.M. Crawford, F. Furche, K. Burke, in *Computational Inorganic and Bioinorganic Chemistry*, edited by E.I. Solomon, R.B. King, and R.A. Scott (Wiley, Chichester, 2009).

- ⁹ *Some Fundamental Issues in Ground-State Density Functional Theory: A Guide for the Perplexed*, J.P. Perdew, A. Ruzsinszky, L.A. Constantin, J. Sun, and G.I. Csonka, J. Chem. Theory Comput. **5**, 902 (2009).
- ¹⁰ *Edge Electron Gas*, W. Kohn and A.E. Mattsson, Phys. Rev. Lett. **81**, 3487 (1998).
- ¹¹ *Eine Verallgemeinerung der Quantenbedingungen für die Zwecke der Wellenmechanik*, G. Wentzel, Zeit. f. Phys. **38**, 518 (1926).
- ¹² *Wellenmechanik und halbzahlige Quantisierung*, H.A. Kramers, Zeit. f. Phys. **39**, 828 (1926).
- ¹³ *La mécanique ondulatoire de Schrödinger: une méthode générale de résolution par approximations successives*, L. Brillouin, Comptes Rendus de l'Académie des Sciences **183**, 24 (1926).
- ¹⁴ *Quantum density oscillations in an inhomogeneous electron gas*, W. Kohn and L.J. Sham, Phys. Rev. **137**, A1697 (1965).
- ¹⁵ *Periodic Orbits and Classical Quantization Conditions*, M.C. Gutzwiller, J. Math. Phys. **12**, 343 (1971).
- ¹⁶ *Density-functional thermochemistry. III. The role of exact exchange*, A.D. Becke, J. Chem. Phys. **98**, 5648 (1993).

- ¹⁷ *Generalized gradient approximation made simple*, J.P. Perdew, K. Burke, and M. Ernzerhof, Phys. Rev. Lett. **77**, 3865 (1996); **78**, 1396 (1997) (E).
- ¹⁸ *Semiclassical Origins of Density Functionals*, P. Elliott, D. Lee, A. Cangi, and K. Burke, Phys. Rev. Lett. **100**, 256406 (2008).
- ¹⁹ C.M. Bender and S.A. Orszag, *Advanced Mathematical Methods for Scientists and Engineers* (Springer-Verlag, New York, 1999).
- ²⁰ H.A. Nayfeh, *Perturbation Methods* (John Wiley & Sons, New York, 1973).
- ²¹ *Asymptotic Expansions of the Dirac Density Matrix*, R. Grover, J. Math. Phys. **7**, 2178 (1966).
- ²² *Asymptotic Evaluation of the Green's Function for Large Quantum Numbers*, R. Balian and C. Bloch, Ann. Phys. **63**, 592 (1971).
- ²³ *Quantum path integrals and reduced fermion density matrices: One-dimensional noninteracting systems*, J.C. Light and J.M. Yuan, J. Chem. Phys. **58**, 660 (1973).
- ²⁴ *Reduced fermion density matrices. II. Electron density of Kr*, J.M. Yuan, S.Y. Lee, and J.C. Light, J. Chem. Phys. **61**, 3394 (1974).
- ²⁵ *Uniform semiclassical approximation to the electron density distribution*, S.Y. Lee and J.C. Light, J. Chem. Phys. **63**, 5274 (1975).
- ²⁶ *Semiclassical density functional theory: Strutinsky energy corrections in quantum dots*, D. Ullmo, T. Nagano, S. Tomsovic, and H.U. Baranger, Phys. Rev. B **63**, 125339 (2001).
- ²⁷ *Landau Fermi-liquid picture of spin density functional theory: Strutinsky approach to quantum dots*, D. Ullmo, H. Jiang, W. Yang, and H.U. Baranger, Phys. Rev. B **70**, 205309 (2004).
- ²⁸ *Restoring the Density-Gradient Expansion for Exchange in Solids and Surfaces*, J.P. Perdew, A. Ruzsinszky, G.I. Csonka, O.A. Vydrov, G.E. Scuseria, L.A. Constantin, X. Zhou, and K. Burke, Phys. Rev. Lett. **100**, 136406 (2008).
- ²⁹ *Accuracy of Approximate Kinetic Energy Functionals in the Model of Kohn-Sham Equations with Constrained Electron Density: the FH...NCH complex as a Test Case*, T.A. Wesolowski, H. Chermette, and J. Weber, J. Chem. Phys. **105** 9182 (1996).
- ³⁰ V.L. Lignères and E.A. Carter, *An Introduction to Orbital-Free Density Functional Theory* (Springer: Netherlands, 2005).
- ³¹ D. Griffiths, *Introduction to Quantum Mechanics*, 2nd ed. (Benjamin Cummings, San Francisco, 2004).
- ³² *Recursion representation of gradient expansion for free fermion ground state in one dimension*, L. Samaj and J.K. Percus, J. Chem. Phys. **111**, 1809 (1999).
- ³³ *On the Connection Formulas and the Solutions of the Wave Equation*, R.E. Langer, Phys. Rev. **51**, 669 (1937).
- ³⁴ *Kinetic energy density and Pauli potential: dimensionality dependence, gradient expansions and non-locality*, A. Holas, P.M. Kozłowski, and N.H. March, J. Phys. A. **24**, 4249 (1991).
- ³⁵ R.M. Dreizler and E.K.U. Gross, *Density Functional Theory* (Springer-Verlag, Berlin, 1990).
- ³⁶ *The Relation between the Wentzel-Kramers-Brillouin and the Thomas-Fermi Approximations*, N.H. March and J.S. Plaskett, Proc. Roy. Soc. (London) **A232**, 419 (1956).
- ³⁷ *Potential Functionals: Dual to Density Functionals and Solution to the v -Representability Problem*, W. Yang, P.W. Ayers, and Q. Wu, Phys. Rev. Lett. **92**, 146404 (2004).
- ³⁸ *Adiabatic Connection and the Kohn-Sham variety of Potential-Functional Theory*, E.K.U. Gross and C.R. Proetto, J. Chem. Theory Comput. **5**, 844 (2009).
- ³⁹ *Condition on the Kohn-Sham kinetic energy, and modern parametrization of the Thomas-Fermi density*, D. Lee, L.A. Constantin, J.P. Perdew, K. Burke, J. Chem. Phys. **130**, 034107 (2009).
- ⁴⁰ *Thomas-Fermi model: The leading correction*, J. Schwinger, Phys. Rev. A **22**, 1827 (1980).
- ⁴¹ *Thomas-Fermi model: The second correction*, J. Schwinger, Phys. Rev. A **24**, 2353 (1981).
- ⁴² *Relevance of the slowly-varying electron gas to atoms, molecules, and solids*, J.P. Perdew, L.A. Constantin, E. Sagvolden, and K. Burke, Phys. Rev. Lett. **97**, 223002 (2006).
- ⁴³ *Non-empirical 'derivation' of B88 exchange functional*, P. Elliott and K. Burke, Can. J. Chem. **87**, 1485 (2009).
- ⁴⁴ *Handbook of Mathematical Functions*, eds. M. Abramowitz and I.A. Stegun (Dover, New York, 1972).